

## **General Disclaimer**

### **One or more of the Following Statements may affect this Document**

- This document has been reproduced from the best copy furnished by the organizational source. It is being released in the interest of making available as much information as possible.
- This document may contain data, which exceeds the sheet parameters. It was furnished in this condition by the organizational source and is the best copy available.
- This document may contain tone-on-tone or color graphs, charts and/or pictures, which have been reproduced in black and white.
- This document is paginated as submitted by the original source.
- Portions of this document are not fully legible due to the historical nature of some of the material. However, it is the best reproduction available from the original submission.

THEORY OF SPECTRAL RADIANCE OF POLLUTANTS AT SEA

Semi-Annual Report  
Under Grant NSG 1528

(NASA-CR-157959) THEORY OF SPECTRAL  
RADIANCE OF POLLUTANTS AT SEA Semi-annual  
Report (University of Southern California)  
45 p HC A03/MF A01 CSCI 13B

N79-18477

Unclas  
G3/45 16085



Prepared for: NASA  
Langley Research Center

Prepared by: The University of Southern California  
Institute for Marine and Coastal Studies  
University Park  
Los Angeles, California 90007

November, 1978

## TABLE OF CONTENTS

FIGURES	<u>Page</u>
1.0      FUNDAMENTALS	ii 2
1.1 <u>Irradiance</u>	2
1.2 <u>Radiance</u>	4
1.3 <u>Diffuse Reflectance</u>	12
1.3.1 <u>Reflectance of Pollutants</u>	13
1.3.2 <u>Diffuse Spectral</u> <u>Reflectance (Color) of</u> <u>Clean Seawater</u>	15
1.4 <u>Sky Reflection</u>	17
1.5 <u>Transmission</u>	25
1.5.1 <u>Polluting Layer</u>	25
1.5.2 <u>Surface Transmission</u>	28
2.0      REMOTE SENSING EQUATIONS	30
2.1 <u>Low Altitude</u>	30
2.2 <u>High-Altitude Sensor, Especially</u> <u>Satellite</u>	36
REFERENCES	40

## FIGURES

Fig. 1. Irradiometer

Fig. 2. Refraction at the sea surface

Fig. 3. Comparison between spectral distribution of downward (—) and upward (---) irradiance for a solar elevation of 55-60° in the Sargasso Sea. (Lundgren and Hojerslev, Kobenhavns Universitet, Rep. Inst. Fys. Oceanog. 14 (1971))

Fig. 4. Compilation of irradiance data by G.L. Clarke and G.D. Ewing, Chapter 17 in Ref. 2. Spectral of the energy of upwelling light on 13 August 1969 in Buzzards Bay at the altitudes shown (measured by TRW spectrometer) and at 0.20 m below the sea surface (measured by Scripps spectrometer) as compared with downwelling irradiance of the NASA Standard spectrum outside the atmosphere, and the downwelling irradiance measured on 14 August 1969 at the sea surface. For the "above surface" curve see text. The energy scale on the right is for downwelling light; that on the left is in relative units, except that the values on the left also represent  $10^{-2} \text{ W/m}^2/\text{nm}$  for the upwelling light at 0.20 m.

Fig. 5. Imaging radiometer

Fig. 6. Upwelling spectral radiance just below the surface computed from measurements at depths of 2.2 and 7.7 m.

- Fig. 7. Component parts of the upwelling radiance signal,  $L_2$ .
- Fig. 8. Computed apparent spectral radiance of the ocean (and its components) as observed above the atmosphere. Blue-green water.
- Fig. 9. Computed apparent spectral radiance of the ocean (and its components) as observed above the atmosphere. Blue water.
- Fig. 10. Computed apparent spectral radiance of the ocean (and its components) as observed above the atmosphere. Green water.
- Fig. 11. Diffuse reflectance.
- Fig. 12. Single scatter event.
- Fig. 13. Apparatus for measuring diffuse reflectance of pollutants.
- Fig. 14. Attenuation curves in the near ultraviolet and in the visible part of the spectrum.  $s$  is total scattering coefficient for pure water and pure sea water as a function of wavelength. Data compiled by A. Morel, Chapter 1 in Ref. 2.
- Fig. 15. Attenuation curve for water between 0.2 and  $2.8\mu\text{m}$ , compiled by A. Morel, Chapter 1 in Ref. 2.
- Fig. 16. Geometry of polarized sky reflection.
- Fig. 17. Reflectance of undisturbed air/water boundary for polarized light ( $r$  and  $r$ ) and for unpolarized light ( $r$ ).

- Fig. 18. Reflectance and transmittance of water/air boundary as a function of the angle of observation for several windspeeds. Curves at left are for radiance coming up from below the surface; those on the right are for radiance incident from above [Ref. 4.].
- Fig. 19. Sky luminance distributions in sun-zenith plane for several locations and solar zenith angles,  $\theta_s$ . Data compiled by Austin [Ref. 3.].
- Fig. 20. Round-trip attenuation.
- Fig. 21. Vertical beam transmittance of the atmospheric models (curves A, B, C, D) and as measured by Guttman (curves a and b). Applied Optics 7 (1968) p. 2377.
- Fig. 22. Absorption cell for measuring pollutant transmittance  $\sqrt{T_p}$ .
- Fig. 23. Quantities for remote sensing equation, low altitude case.
- Fig. 24. Polluted layer over clean seawater.
- Fig. 25. Light from polluted area diluted by scattering.

## THEORY OF SPECTRAL RADIANCE OF POLLUTANTS AT SEA

This report concerns remote measurement of pollutants dumped in the sea, not oil slicks, but soluble pollutants that change the color of the water. The sensor is a spectral radiometer that flies over the polluted area and compares its spectral radiance (color) to that of surrounding clean seawater.. It is fairly easy to make a qualitative determination that a plume of pollutant occupies a certain area. However, the goal here is quantitative, namely to infer the concentration of pollutants using the measured radiance of the sea compared to laboratory measurements of reflection and transmission spectra of the pollutants. Many previous papers and reports have discussed remote sensing of ocean color. The main contribution here is how to use data quantitatively that compare the polluted area to surrounding clean water.

We treat the subject in three steps. The first section defines the quantities involved and describes means for measuring them. The second section derives the equations for remote sensing with a low-flying aircraft, in which case the absorption and radiance of intervening air is negligible. The third section applies to high-flying aircraft and satellites, in which case the radiance of intervening air is the major problem.

## 1.0 FUNDAMENTALS

This section describes measurements of light intensity, reflection, and transmission.

### 1.1 Irradiance

The brightness of the sea surface is proportional to the amount of incident sunlight measured as an irradiance, so much power (watts) per unit area ( $\text{m}^2$ ). This incident light is a combination of collimated direct sunlight and diffuse sky light. The angles of incidence are not too important as long as the sun is fairly high in the sky because refraction at the sea surface bends the rays toward the nadir, Fig. 1, so that all the light is directed more or less downward.

A meter that measures irradiance (irradiometer) is nothing more than a lensless light detector with a precise area  $A$  of detection defined by a mask, Fig. 2. The detector measures power  $P$ , and irradiance is given by

$$H = P/A \quad (1)$$

Since  $A$  is constant, a practical meter is calibrated directly in irradiance units, such as  $\text{watts}/\text{m}^2$ . A suitable antireflection coating on the detector helps to make the meter insensitive to the angle of incidence. To measure light incident on the sea, it is important that the irradiometer be exactly horizontal. Obviously it will intercept more sunlight if tilted toward the sun.

Since we are interested in color of the sea, we need a spectral irradiometer which measures spectral irradiance,  $\text{watts}/\text{m}^2/\text{nm}$ . The irradiometer is converted to a spectral irradiometer by



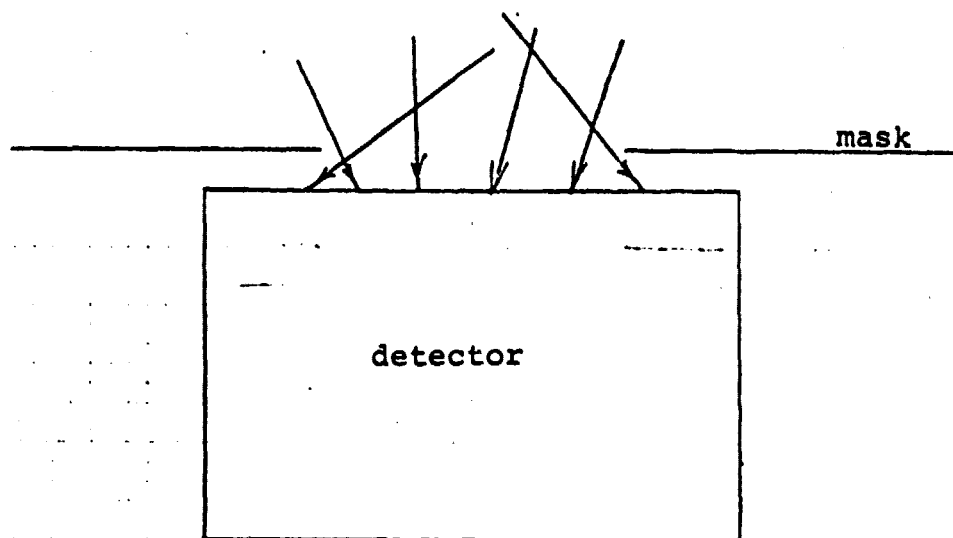


Fig. 1. Irradiometer

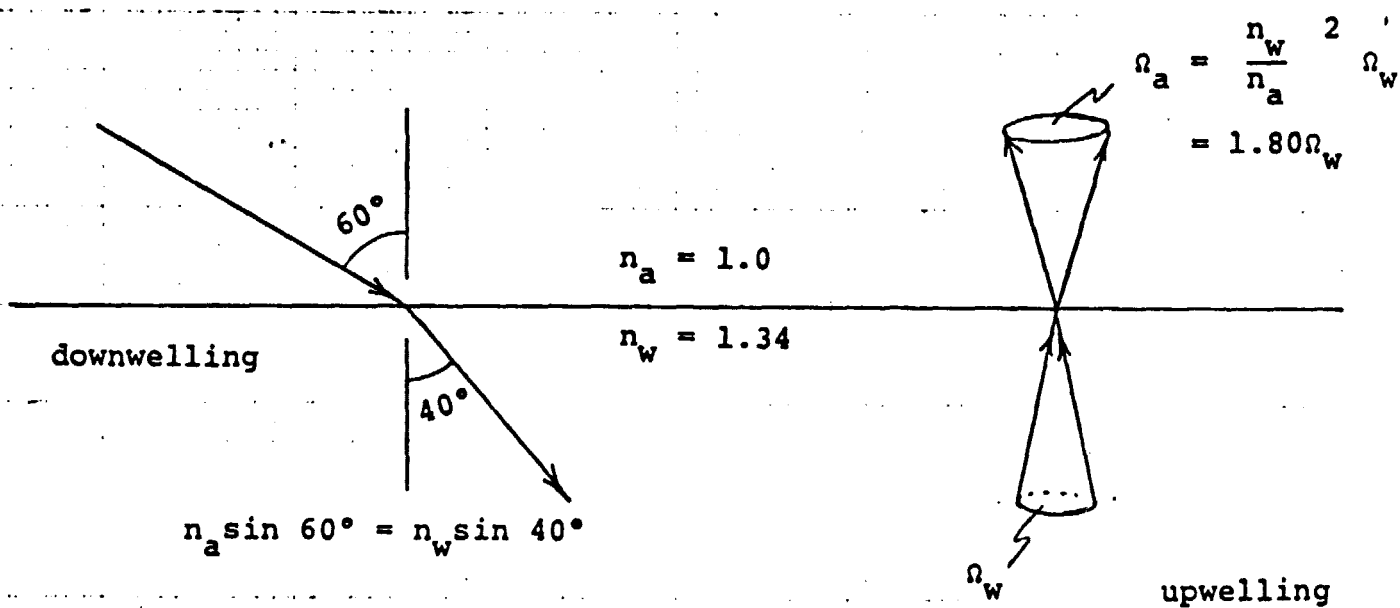


Fig. 2. Refraction at the sea surface

covering it with a series of absorbing filters of bandwidth B. (Interference filters would be sensitive to angle.) Then the spectral irradiance is given by

$$H_{\lambda} = H/B = P/AB \quad (2)$$

Numerous measurements of irradiance have been made and compiled in texts on ocean optics, e.g. Jerlov [Ref. 1] pp 71, 128 (Figs. 63 and 65b), and 144 and Jerlov and Nielsen [Ref. 2] pp 88 and 399. Two summaries of irradiance appear in Figs. 3 and 4. Note that just beneath the surface, downwelling irradiance in the blue-green is about 20 times the upwelling. This ratio increases to 35 in the red. In a later estimate we use the value

$$H(510 \text{ nm}) = 1.2 \text{ W/m}^2/\text{nm}$$

## 1.2 Radiance

The remote sensor that looks at the sea cannot be a lensless irradiator. An imaging sensor is required to distinguish a plume of polluted water from surrounding clean water. The amount of light power this sensor detects from each pixel is proportional to the solid angle of rays that it intercepts, and so the appropriate measure of sea brightness is power (watts) per unit area ( $\text{m}^2$ ) per unit solid angle (steradian), a quantity called radiance, L.

Figure 5 shows the optics in a radiometer. Power received at the detector is given by

$$P = L \times \left( \begin{array}{c} \text{area of resolution cell} \\ \text{Fig. 5, lower right} \end{array} \right) \times \left( \begin{array}{c} \text{solid angle intercepted} \\ \text{Fig. 5, lower left} \end{array} \right)$$

From the geometry, these quantities are evaluated as follows:

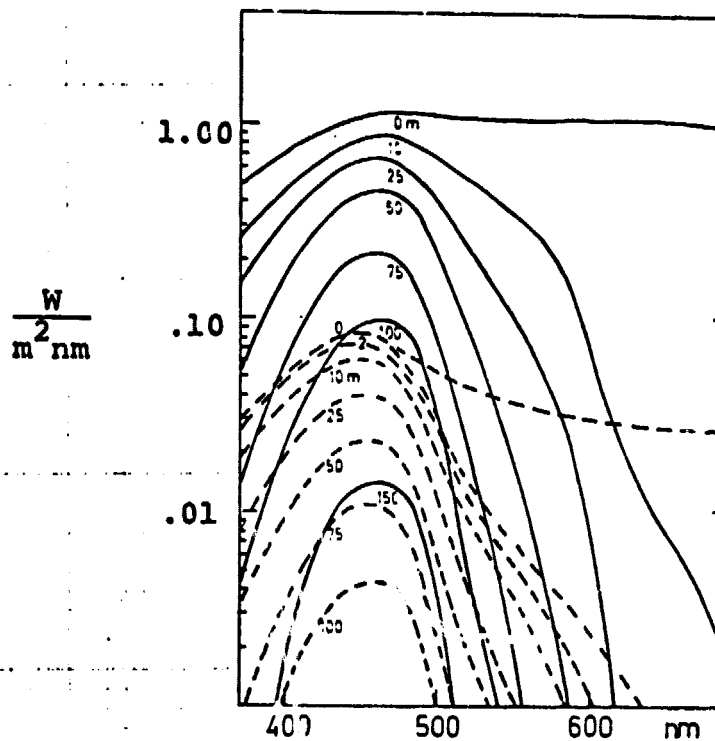


Fig. 3. Comparison between spectral distribution of downward (—) and upward (---) irradiance for a solar elevation of 50-60° in the Sargasso Sea. (Lundgren and Hojerslev, Kobenhavns Universitet, Rep. Inst. Fys. Oceanog. 14 (1971))

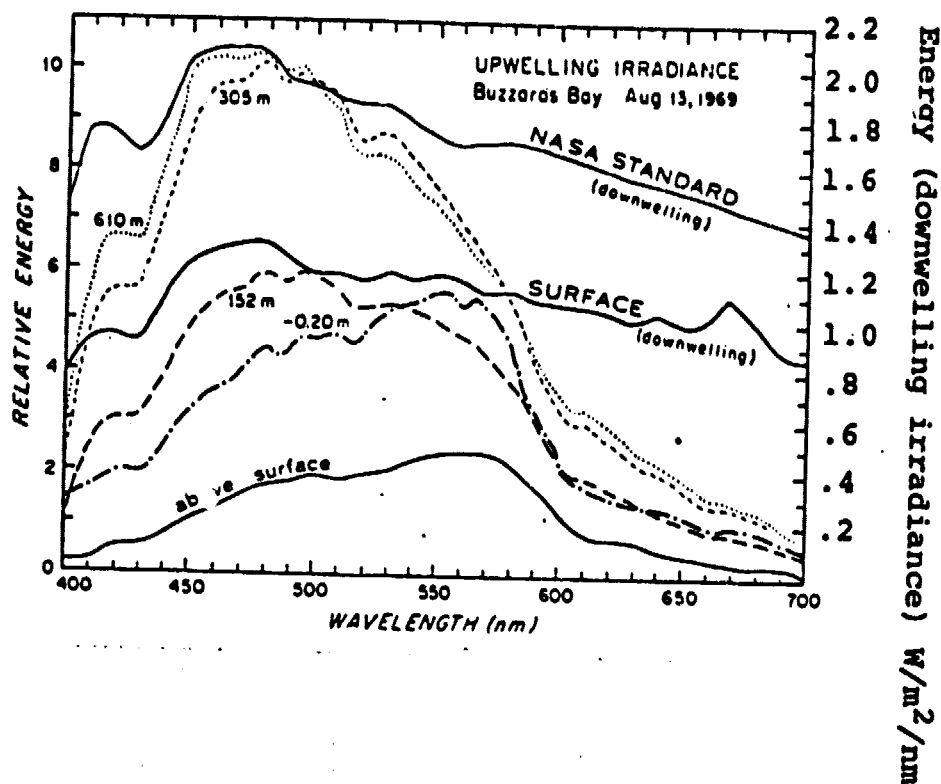


Fig. 4. Compilation of irradiance data by G.L. Clarke and G.C. Ewing, Chapter 17 in Ref. 2. Spectra of the energy of upwelling light on 13 August 1969 in Buzzards Bay at the altitudes shown (measured by TRW spectrometer) and at 0.20 m below the sea surface (measured by Scripps spectrometer) as compared with downwelling irradiance of the NASA Standard spectrum outside the atmosphere, and the downwelling irradiance measured on 14 August 1969 at the sea surface. For the "above surface" curve see text. The energy scale on the right is for downwelling light; that on the left is in relative units, except that the values on the left also represent  $10^{-2} \text{ W/m}^2/\text{nm}$  for the upwelling light at 0.20 m.

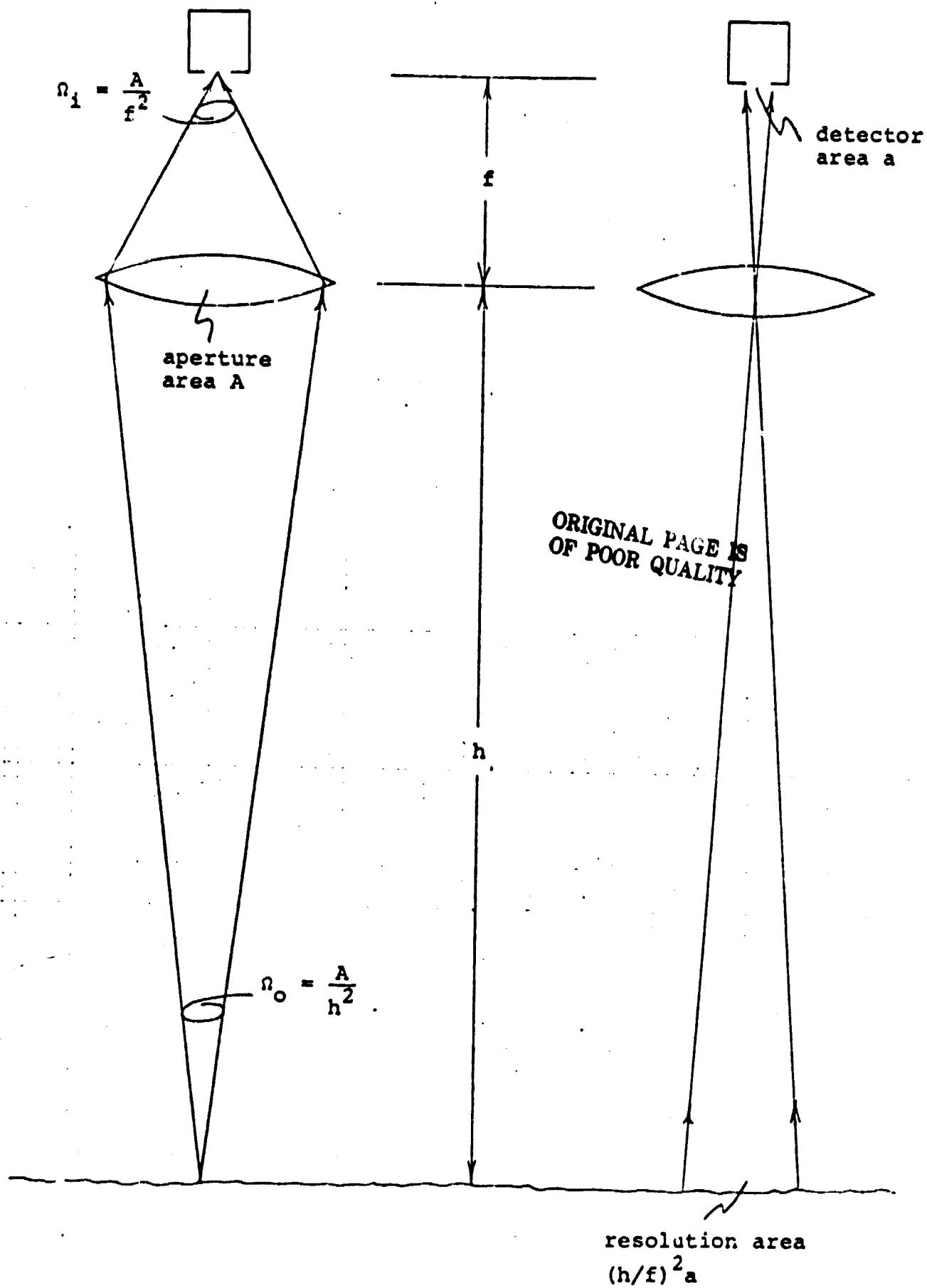


Fig. 5. Imaging radiometer

$$P = L \left( \frac{h^2}{f^2} a \right) \left( \frac{A}{h^2} \right) = L \frac{Aa}{f^2} = \frac{\pi}{4} L \frac{a}{(f/d)^2} \quad (3)$$

where  $A = \pi D^2/4$  is the collecting aperture, and  $D$  its diameter,  $f$  the focal length, and  $h$  the altitude of the sensor. Note that  $h$  drops out, and  $Aa/f^2$  is a constant of the optics. This means that the detector output can be calibrated directly in terms of radiance, watts/m<sup>2</sup>/nm. Also note that the radiance of the image is the same as that of the object, neglecting absorption in the lens:

$$L_i = \frac{P}{\Omega_i a} = \frac{P}{(A/f^2) a} = \frac{Pf^2}{Aa} = L \quad (4)$$

Again we are interested in color of the sea, and so spectral radiance is required:

$$L_\lambda = L/B \quad (5)$$

Absorbing filters could be used, but in this case the optics can be used to collimate light in a suitable way to use a grating or prism monochromator. These details are beyond the scope of this report. From this point on, we drop the subscript  $\lambda$  with the understanding that all radiances and irradiances are spectral.

Austin [Ref. 3] has compiled graphs of radiance that are particularly useful for remote sensing. Four of these appear in Fig. 6 and 8 through 10. Fig. 7 defines the notation he uses. The following features in these data influence the techniques discussed later:

- ▶  $L(510 \text{ nm}) = 0.9 \times 10^{-2} \text{ w/m}^2/\text{sr/nm}$  regardless of the color of the water (Fig. 6)
- ▶ In the deep red, sky radiance reflected by the surface ( $L_r$ ) exceeds that which has penetrated the water ( $L_w$ ). The crossover falls in the range 580 - 650 nm.

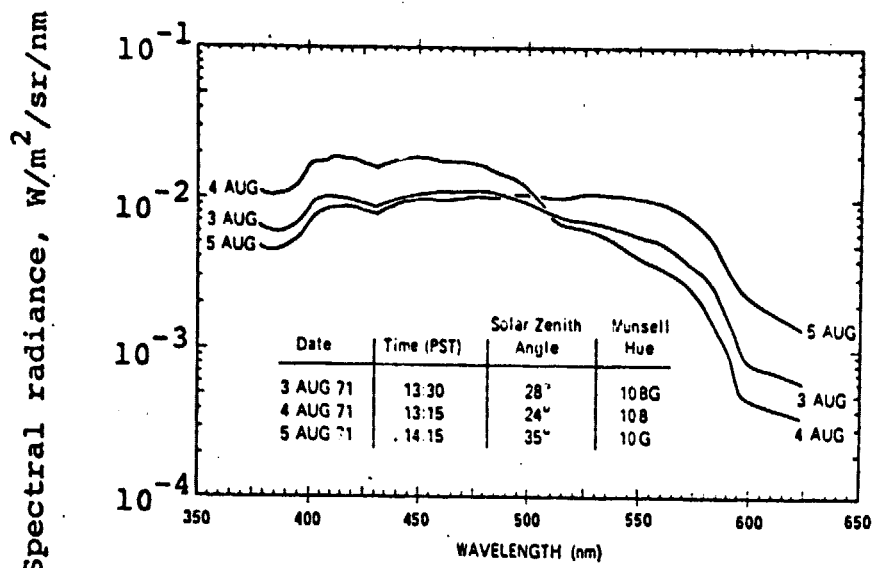


Fig. 6. Upwelling spectral radiance just below the surface computed from measurements at depths of 2.2 and 7.7 m.

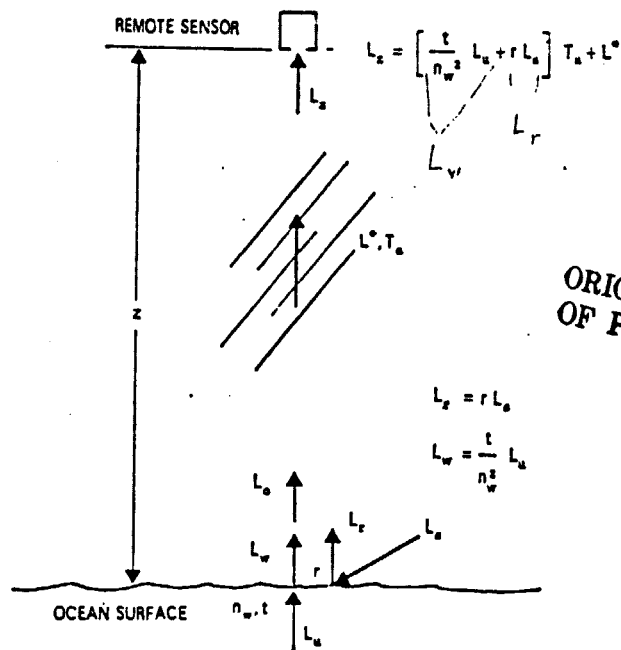


Fig. 7. Component parts of the upwelling radiance signal,  $L_z$ .

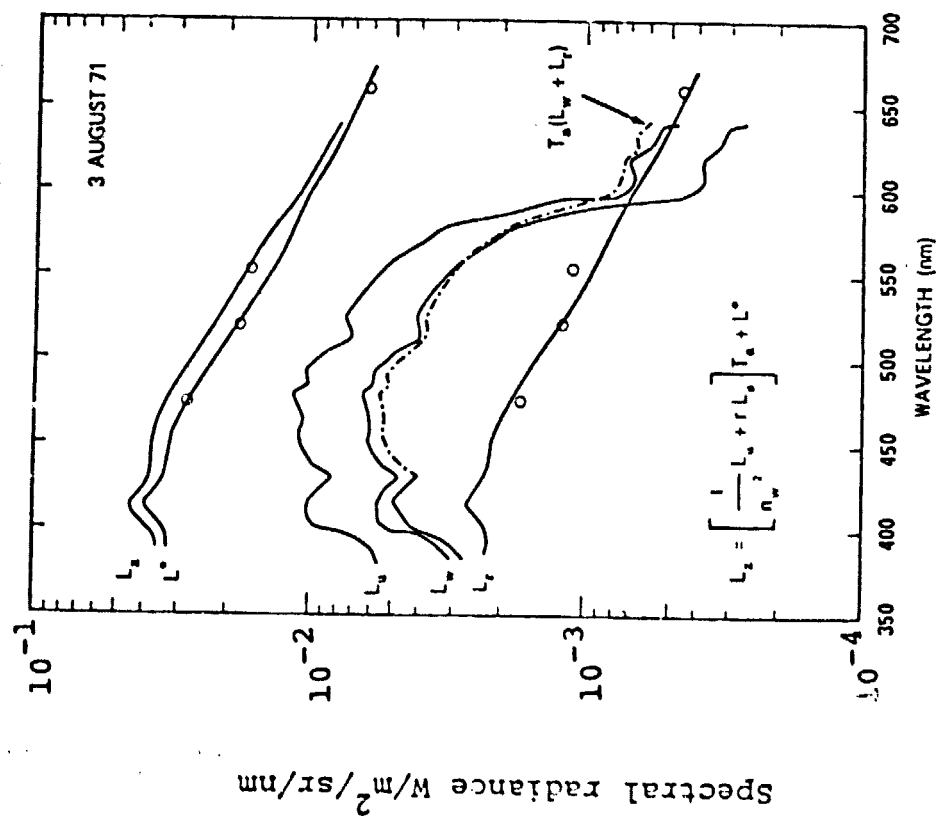


Fig. 8. Computed apparent spectral radiance of the ocean (and its components) as observed above the atmosphere. Blue-green water.

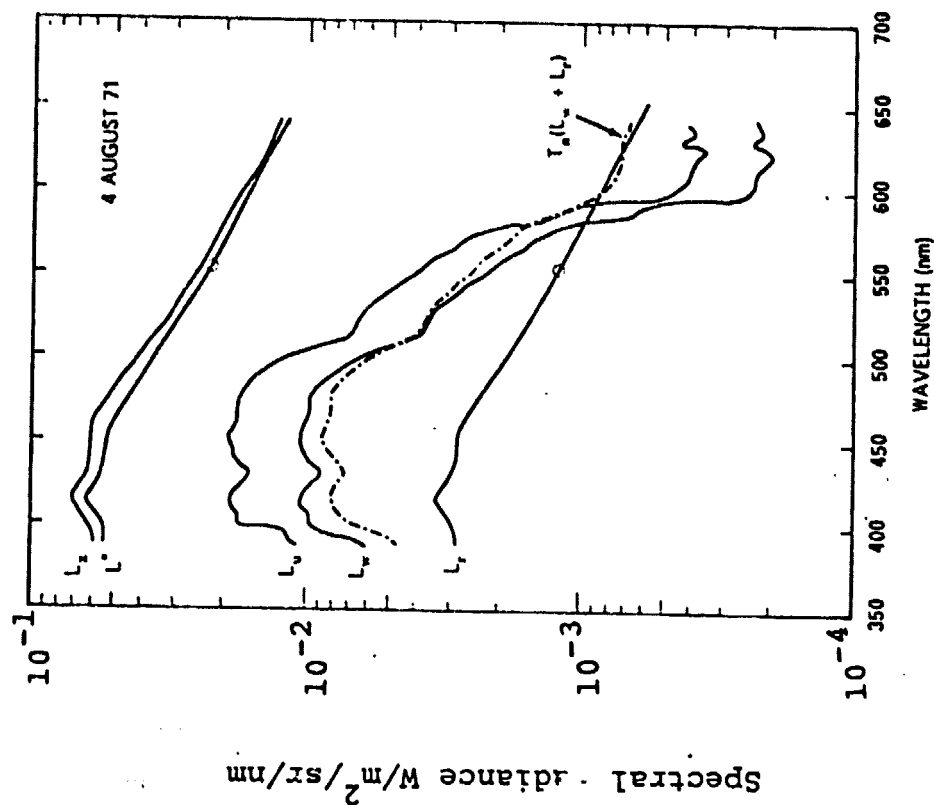


Fig. 9. Computed apparent spectral radiance of the ocean (and its components) as observed above the atmosphere. Blue water.



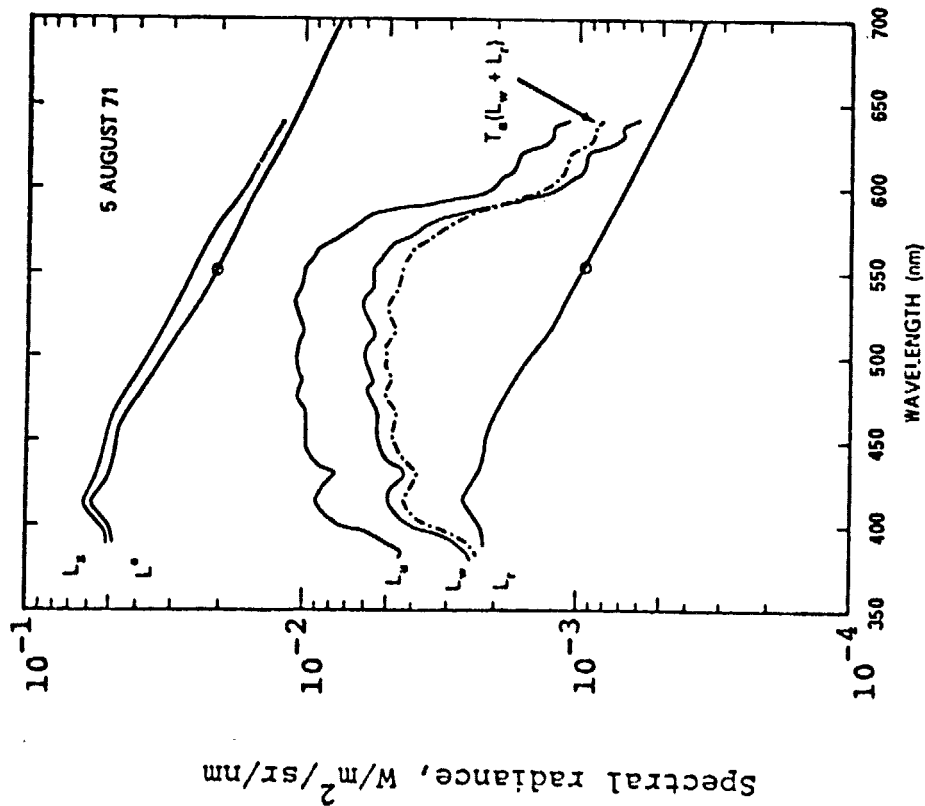


Fig. 10. Computed apparent spectral radiance of the ocean (and its components) as observed above the atmosphere. Green water.

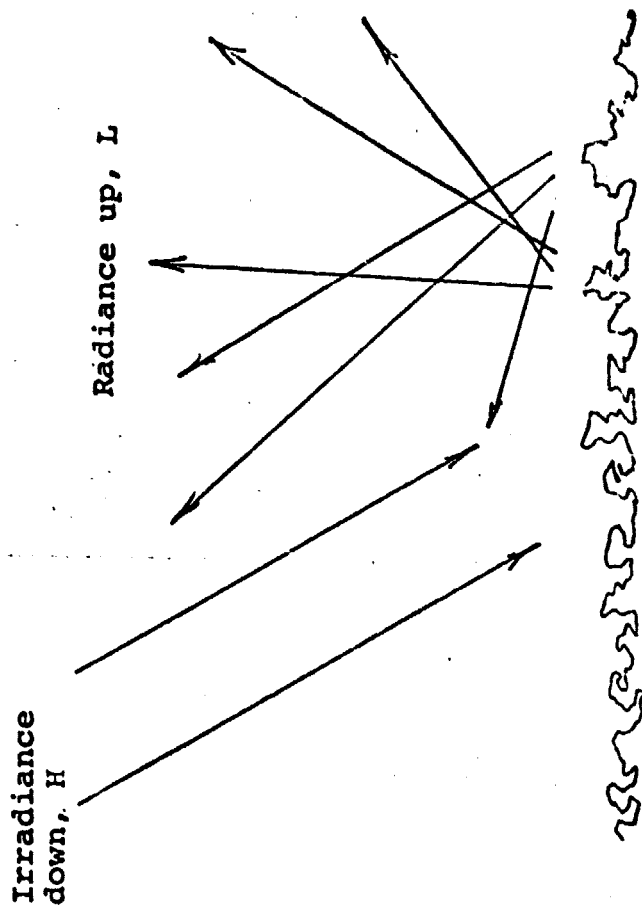


Fig. 11. Diffuse reflectance

- From high altitude or outer space, the observed radiance ( $L_z$ ) is dominated by the veiling luminance of the intervening air ( $L^*$ ).

### 1.3 Diffuse Reflectance

Consider direct sunlight incident on a rough surface as shown in Fig. 11. The ratio of reflected to incident power is reflectance  $\rho$ , a dimensionless quantity. In order to relate  $L$  seen by the radiometer to  $H$ , the incident light, we need the ratio  $L$  to  $H$ , a quantity with dimensions of per steradian:

$$\frac{L}{H} = R = \frac{\rho}{\Omega_{\text{eff}}} \quad (6)$$

where  $\Omega_{\text{eff}}$  is the effective solid angle over which the light is scattered. We call this ratio the diffuse reflectance.\*

Consider the bulk reflectance  $R$  of a liquid, excluding reflection at the surface, which we treat separately. This liquid can

---

\* In the case of a perfectly white diffuse reflector,  $\rho = 1$  and  $\Omega_{\text{eff}} = \pi$ , the effective solid angle for a lambertian (cosine law) surface. Hence  $R_{\text{ideal}} = 1/\pi$ . This relationship provides a means for calibrating a radiometer against an irradiator given a near-perfect surface. For airborne instruments, a cloud bank serves this purpose very well providing it is thick enough to stop direct sunlight (cannot see the sun from below) but not thick enough to be an absorber (dark thunderhead). In this case

$$L_{\text{up}} + L_{\text{down}} = H/\pi \quad (7)$$

where values of  $L$  are measured from above the clouds looking down, and below looking up and for a cloud of the right thickness they are about equal.

be either clean or polluted seawater; in either case it contains particulate matter that reflects light diffusely. It is possible in principle to derive an expression for R using the attenuation  $\alpha$  of the medium and the diffuse reflectance  $\sigma dz$ , Fig. 12, caused by particulate matter (plus Rayleigh scattering) in each infinitesimal layer. A simple expression useful later applies to the case in which the absorption rate,  $a$ , dominates over scattering:

$$a > s = \int_{4\pi} \sigma(\theta) d\omega \text{ or } a > 4\pi\sigma(180^\circ)$$

Multiple scattering is negligible in this case, and the single scatter rays in Fig. 12 lead to the expression

$$R = \int_0^\infty e^{-\alpha z} (\sigma dz) e^{-\alpha z} = \sigma \int_0^\infty e^{-2\alpha z} dz$$

$$R = \sigma/2\alpha, \quad a > 4\pi\sigma(180^\circ) \quad (8)$$

It is possible to treat more general cases, but we see no point in relating R to the bulk optical properties of the liquid. Instead it is more reliable simply to measure reflectance in the laboratory for various concentrations of the polluted layer. This is especially true in view of the fact that some pollutants undergo chemical change as the concentration changes. For example, the acid waste that DuPont dumps precipitates iron when diluted.

### 1.3.1 Reflectance of Pollutants

Figure 13 shows an apparatus suitable for measuring diffuse reflectance. A known irradiance H illuminates a cylindrical column of liquid (thickness z). A radiometer in a side arm measures L, and then

$$RT = L/H \quad (9)$$

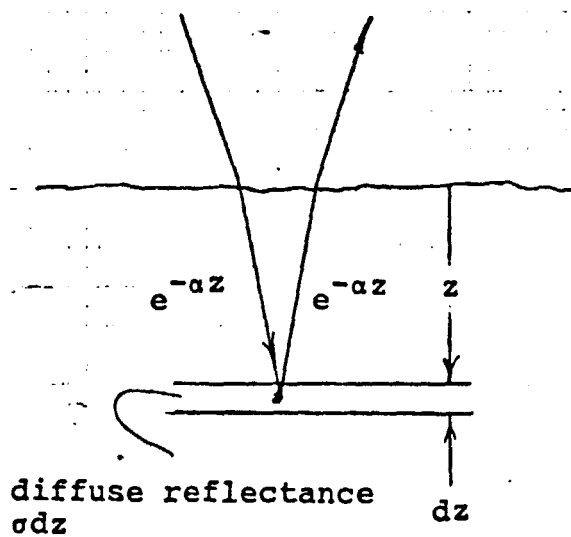


Fig. 12. Single scatter event

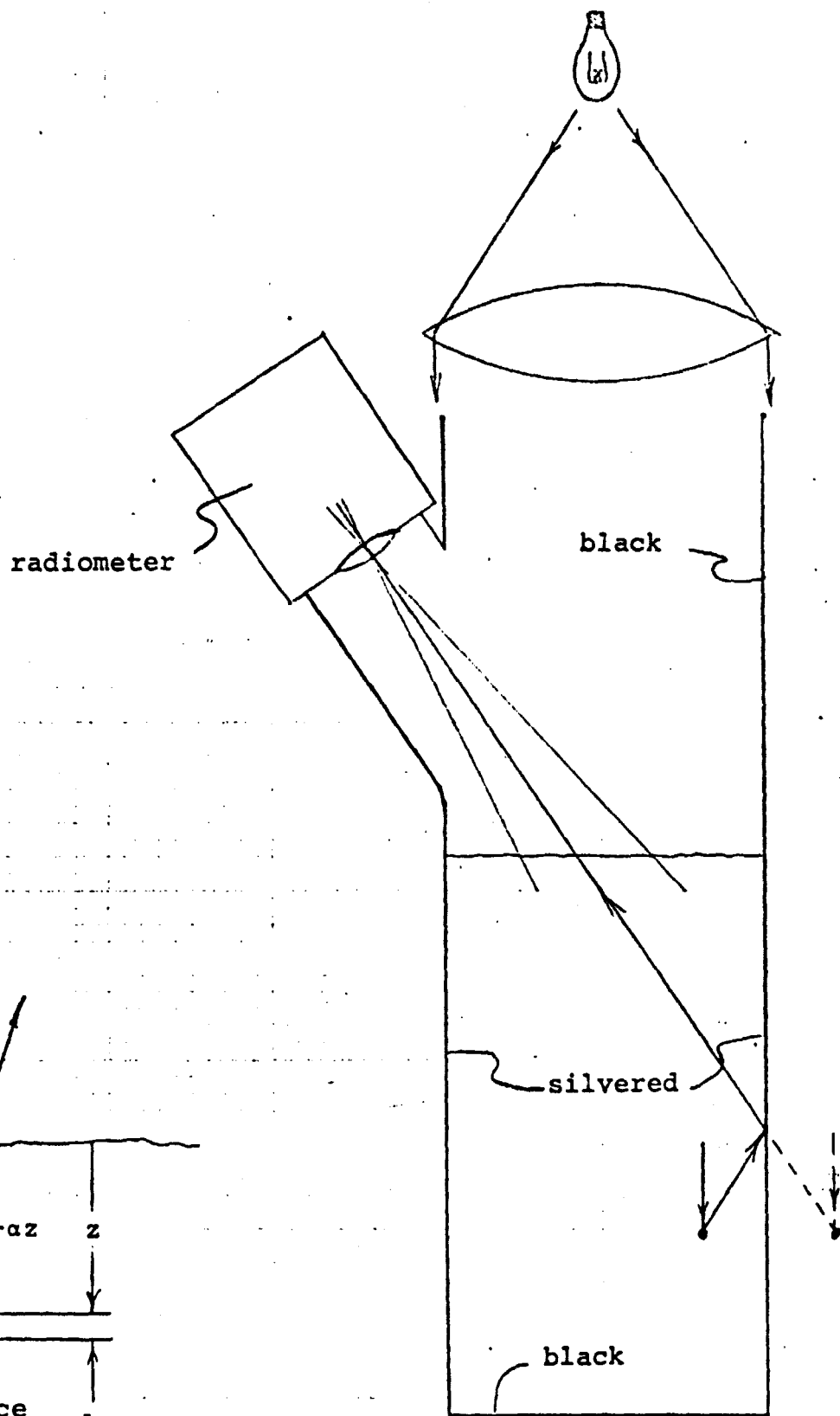


Fig. 13. Apparatus for measuring diffuse reflectance of pollutants

Here T is a transmission factor for the air/liquid dielectric interface (discussed later). It is just as well to measure the product RT instead of each separately, because the product is what appears later in the equations for remote sensing.

Several features of this apparatus (Fig. 13) are noteworthy. First the cylindrical wall below the surface should be highly reflecting, silvered preferably on the inside (and coated to prevent corrosion). This simulates the effect of an unbounded ocean by replacing light that would come from outside the cylinder (dashed ray lower right) by a reflected ray on the inside. Other surfaces should be black to reduce stray light. To avoid edge effects, the incident beam must overfill the cylinder, and the radiometer's field of view must not extend to the side walls.

### 1.3.2 Diffuse Spectral Reflectance (Color) of Clean Seawater

We tend to think that the color of seawater is obvious, somewhere between blue and green, but actually the apparent color is contaminated with a lot of sky reflection, somewhere between blue and white, and the correction is not always straightforward. Probably the only reliable means to measure the true color of seawater alone, i.e.  $R_w$ , its spectrum of diffuse reflectance, in all weather requires a boat trip to the site in question. One measures radiance  $L_u$  (upwelling) with a radiometer just under the surface looking down, and irradiance  $H_d$  (downwelling) with an irradiator just under the surface looking up. Then

$$R_w = L_u / H_d$$

In a few sites where pollutants are dumped regularly, it may be practical to do this enough times to establish the variations

of  $R_w$  with season, hour of the day, and sea state. Then, from that time on,  $R_w$  may be considered a known spectrum in the remote sensing equation.

Obviously we need a fall-back position for areas that do not justify all that labor. One alternative is to fly over the areas and take measurements when the sea is calm and the sky uniform. Under these circumstances, the remote sensing equation (Eq. 17, discussed later) may be solved for  $R_w$  since all other quantities are either known or easily measurable. One has to hope that the values of  $R_w$  found in this way also hold when the weather changes.

The final fall-back position is to use only two colors where  $R_w$  is fairly invariant from place to place and therefore known. These values are

$$\left. \begin{array}{l} \text{Green: } R_w(510 \text{ nm}) = 8 \times 10^{-3} \text{ sr}^{-1} \\ \text{Near infrared: } R_w(700 \text{ to } 1100 \text{ nm}) = 0 \end{array} \right\} \quad (10)$$

These numbers require some explanation. The green color is where blue water, blue-green water, and green water all have the same reflectance, Fig. 6. This assumes that the water in question is moderately deep and its color is not influenced by bottom reflection, silt, or gelbstoff. Unfortunately we know of no case in which  $R_w(510 \text{ nm})$  or any other wavelength has been measured directly. We calculated the value above from a ratio  $L/H$  in which  $L$  and  $H$  were typical values measured in widely different parts of the world by different groups who presumably do not compare instruments. We took  $L$  from Fig. 6 and  $H$  is an average from Figs. 3, 4, and others like

them. This situation should be corrected because any quantity that is fairly invariant should be pinned down and published as a universal semi-constant whose range of variation is known.

The second of Eqs. 10,  $R_w(700 \text{ to } 1100) = 0$ , simply means that  $R_w$  is negligible. To estimate the actual value, let us use Eq. 8 with

$$\begin{aligned}\sigma(160^\circ) &= 10^{-3} \text{ per meter per steradian} \\ a = \alpha &= 0.5 \text{ per meter.}\end{aligned}$$

The former avoids a fairly sharp peak at  $180^\circ$  and represents a fairly large value of the scattering function in a backward direction. The value of the attenuation constant  $\alpha$  comes from Fig. 14. Now Eq. 8 gives

$$R = \sigma/2\alpha = 10^{-3} \text{ per steradian,}$$

an order of magnitude less than the green value, which already represents a very dark scattering medium. (Deep seawater looks almost black compared to most diffuse reflectors.) The useful range of infrared cuts off at about 1100 nm where light penetrates only about a centimeter of water, Fig. 15, hardly enough to see an appreciable amount of diluted pollutant.

In view of the difficulties in determining  $R_w$ , it is advisable to formulate the remote sensing equations in such a way that this quantity drops out. This is done in Sec. 2, but the result is not usable in all circumstances.

#### 1.4 Sky Reflection

Reflections from fog, foam, spray and particulates in the sea are all of the diffuse type described in the preceding section. There is one exception, reflection at a calm sea surface.

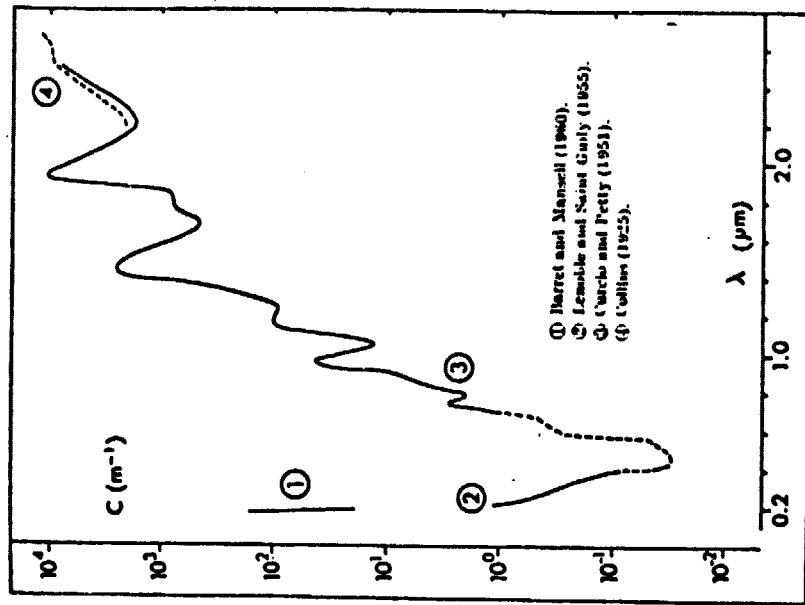


Fig. 14. Attenuation curves in the near ultraviolet and in the visible part of the spectrum

▲ Lenoble-Saint Guily (1955), path length: 400 cm;  
 x x Halbut (1934) (1945), path length: 364 cm;  
 ● Sullivan (1963), path length: 132 cm;  
 O— Clarke-James (1939), path length: 97 cm (Ceresin lined tube);  
 O... James-Burge (1938), path length: 97 cm (Silver lined tube).

s is total scattering coefficient for pure water and pure sea water as a function of wavelength. Data compiled by A. Morel, Chapter 1 in Ref. 2.

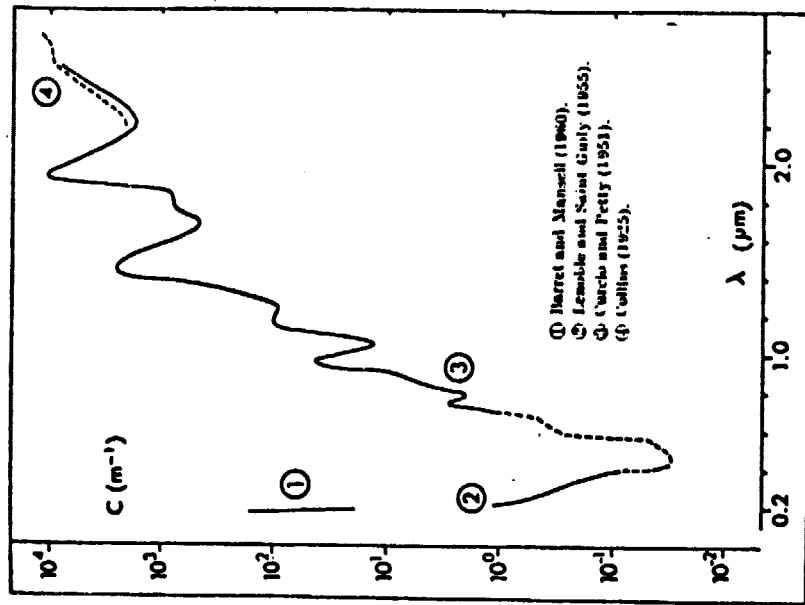


Fig. 15. Attenuation curve for water between 0.2 and 2.8  $\mu\text{m}$ , compiled by A. Morel, Chapter 1 in Ref. 2.

ORIGINAL  
 OF POOR QUALITY



This is a simple specular reflection with no angular spread, and so collimated direct sunlight is still collimated after reflection, and the radiometer sees a reflected image of the sun. The brilliance of this image is overpowering and masks the color of the sea. Any radiometer looking down at the sea must be pointed away from the sun's image to obtain useful data. With this precaution, the downlooking radiometer sees the color of the sea, but it is still contaminated by a significant amount of reflected sky radiance:

$$L_r = rS$$

where  $S$  is the radiance of the sky as measured looking up at the angle supplementary to the direction of  $L_{sk}$  as Fig. 16 shows. The extent of this contamination is considerable:  $L_r$  is about 1/3 of the desired radiance  $L_w$  from the water (Figs. 8, 9, and 10) throughout most of the spectrum, but the two cross over in red and the contamination exceeds the signal. Since no angular spreading occurs at reflection, and both  $L_{sk}$  and  $S$  have spectral radiance units ( $W/m^2/sr/nm$ ), it follows that  $r$  is a dimensionless number like the reflectivity of any mirror surface.

Values of  $r$  are plotted in Fig. 17, which shows that it is dependent on polarization, the symbol " $\perp$ " referring to polarization (E-vector) perpendicular to the plane of incidence and " $\parallel$ " to polarization in the plane of incidence. Since skylight is also polarized, the equation above becomes two equations:

$$\begin{aligned} L_r^\perp &= r_\perp S_\perp \\ L_r^\parallel &= r_\parallel S_\parallel \end{aligned} \tag{11}$$

For small angles, i.e. directions within about  $20^\circ$  of nadir,

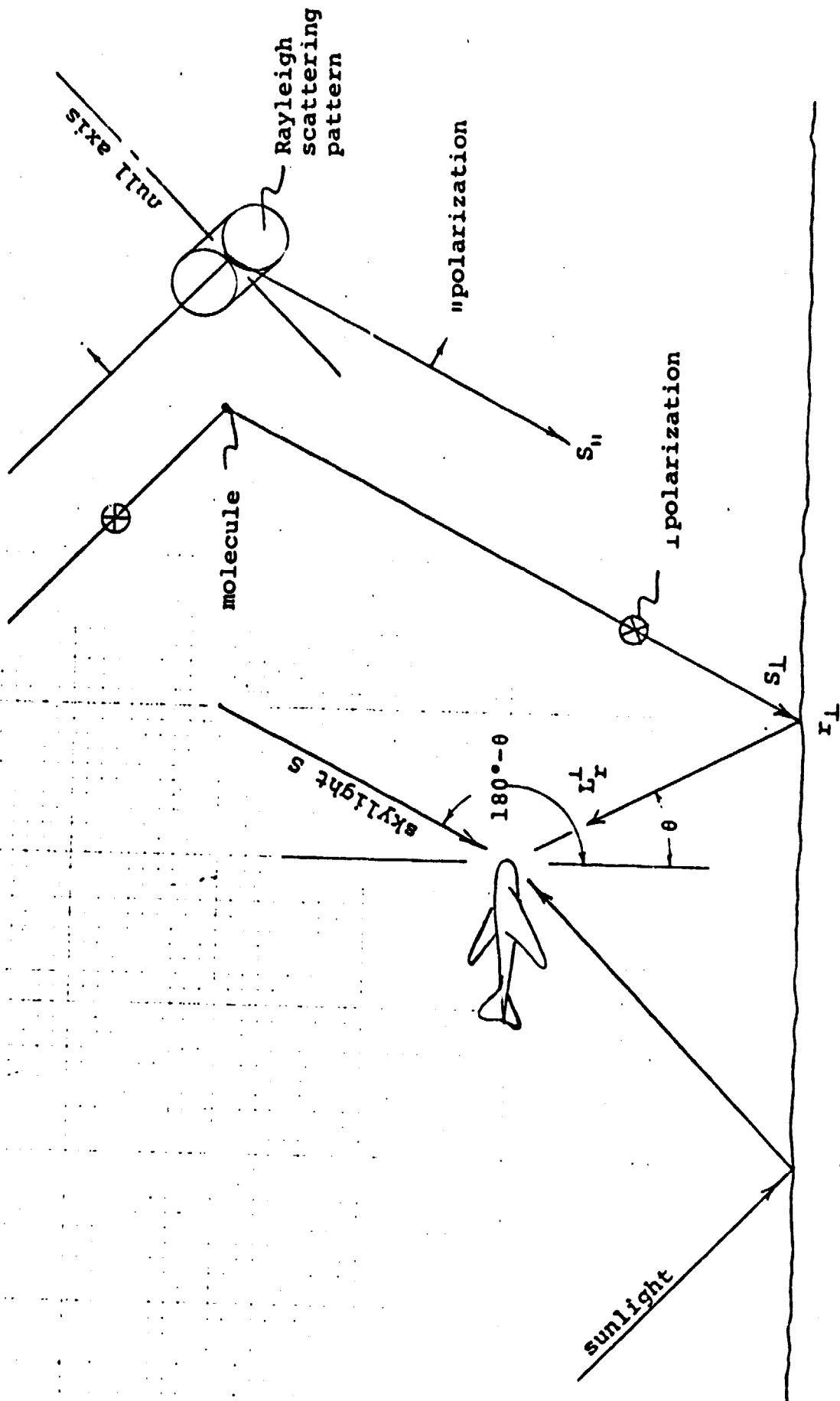


Fig. 16. Geometry of polarized sky reflection

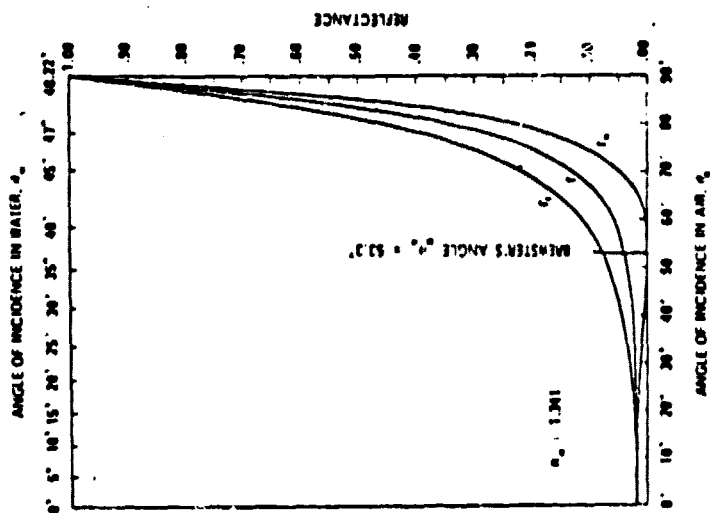


Fig. 17. Reflectance of undisturbed air/water boundary for polarized light ( $r_p$  and  $r_u$ ) and for unpolarized light ( $r$ ).

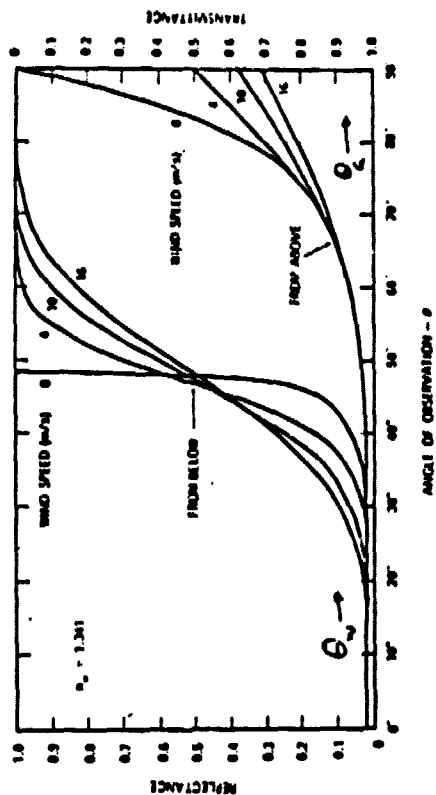
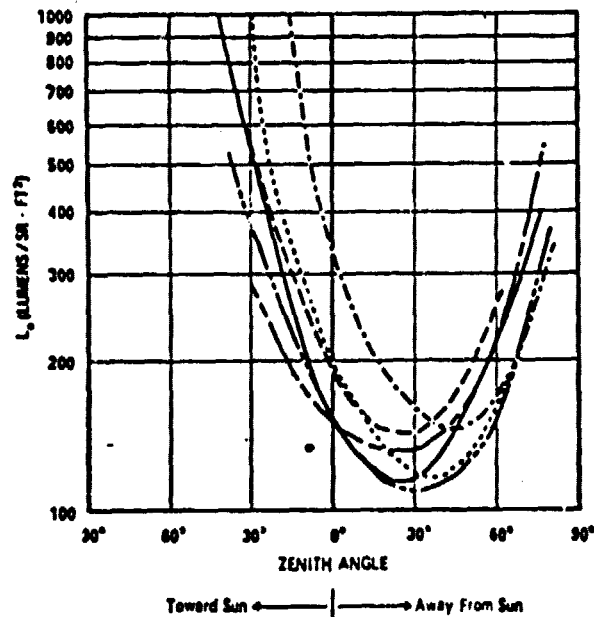


Fig. 18. Reflectance and transmittance of water/air boundary as a function of the angle of observation for several wind speeds. Curves at left are for radiance coming up from below the surface; those on the right are for radiance incident from above. [Ref. 4.]

$\theta_s$	DATE	PLACE	REFERENCE
24°	6-2-67	San Diego	Vis Lab
38°	6-2-67	San Diego	Vis Lab
43°	10-7-69	San Diego	Vis Lab
50°	5-1947	Bocaiuva	Richardson & Mulbert (1949)
52°	9-2-64	San Diego	Vis Lab
67°	10-2-53	Stockholm	Hopkinson (1954)



ORIGINAL PAGE  
OF POOR QUALITY

Fig. 19. Sky luminance distributions in sun-zenith plane for several locations and solar zenith angles,  $\theta_s$ . Data compiled by Austin [Ref. 3].

the reflectivity is given by

$$r_{\parallel} = r_{\perp} = \left( \frac{n_w - n_a}{n_w + n_a} \right)^2 = 2.1\% \quad (12)$$

the well-known Fresnel formula for dielectric reflection at normal incidence in which  $n_w = 1.341$  is the refractive index of seawater and  $n_a = 1.0$  is that of air.

At other angles  $r$  is given by formulas that are straightforward but complicated and are given in numerous physics and optics texts. They are of little if any practical value here because the sea surface is ruffled by wind which averages the reflectivity over a range of angles. Gordon [Ref. 4] has computed the average for various wind speeds with the results given in Fig. 18.

The wind-ruffled sea surface blurs the reflected image of the sun into a glittering pattern called sun glint. The radiometer should be pointed away from the sun to avoid this glint as much as possible, Fig. 16. However, to reduce sky contamination to a minimum, the radiometer should look somewhat farther from the reflected sun angle, as Fig. 19 shows, about  $75^\circ$  when the sun is high in the sky to  $90^\circ$  when it is low.

By coincidence, this same direction gives the maximum polarization of reflected skylight in the perpendicular direction due to both factors in Eq. 11:

$$r_{\perp} > r_{\parallel} \text{ and } S_{\perp} > S_{\parallel}$$

The former fact is apparent from Fig. 17 and the latter results from the dipole radiation pattern of molecular scatter shown in Fig. 16. Unfortunately Fig. 18 is computed for unpolarized light and we do not have a similar one for the separate components.

When the sky is mostly clear, so that light has the directional qualities shown in Fig. 16, then the radiometer should be pointed to avoid reflected skylight and a polarization analyzer should be used to reject the perpendicular component. The radiometer's field of view should be centered about a direction 75 to 90° away from the reflected sun image in the plane containing that image and the nadir. This technique gives four advantages:

- ▶ Avoids sun glint
- ▶ Rejects sky contamination by looking at the darkest part
- ▶ Further rejects skylight by taking advantage of its polarization
- ▶ Takes further advantage of the polarization by Fresnel reflection.

If the sky is clear (so that molecular scattering dominates over particle scattering), then a polarization filter almost completely eliminates sky reflection at the longer wavelengths.\* This is fortunate, because it normally causes most of the veiling luminance at the longer wavelengths; compare  $L_r$  and  $L_w$  in Figs. 8, 9, and 10.

---

\*Some blue and violet remain, which have been depolarized by double scattering in the atmosphere, but this falls off as  $\lambda^{-8}$ , a factor of  $\lambda^{-4}$  for each of two Rayleigh scatters. This is why the sky looks violet in some photos taken through polaroid at right angles to the sun.

## 1.5 Transmission

We shall use transmission factors  $T$  to account for loss of light in propagating through lossy media:

$T_a$  - atmosphere (satellite case)

$T_s$  - sea surface

$T_p$  - polluted layer

In every case, light that passes down through a layer must return through the same layer to be detected, and so we use capital  $T$  to represent round-trip propagation. However, this does not imply that the loss is the same each way. For example, when the sun is rather far off the zenith, Fig. 20, and the radiometer is looking straight down, the transmittance through some layer going down is  $\tau = e^{-\alpha(z_a \sec \theta)}$  while going up it is considerably less, namely  $\tau = e^{-\alpha z_a}$ ; hence,

$$T = \tau \tau = \exp [-\alpha z_a (1 + \sec \theta)] \quad (13)$$

In estimating  $T$ , light that is scattered through small angles should not be counted as lost. A cutoff angle is not easy to define, and will have to be determined by empirical matches to the remote sensing equations using data taken at sea. Fig. 21 shows a summary of estimates of the unscattered transmittance of the atmosphere needed for the case of a satellite sensor.

### 1.5.1 Polluting Layer

For measuring  $\sqrt{T_p}$  a suitable absorption cell is shown in Fig. 22. The inside cylindrical wall is silvered for the same reason discussed in connection with Fig. 13. Similarly, the known incident irradiance overfills the stop aperture, and the detector is large enough to catch all light at the output.

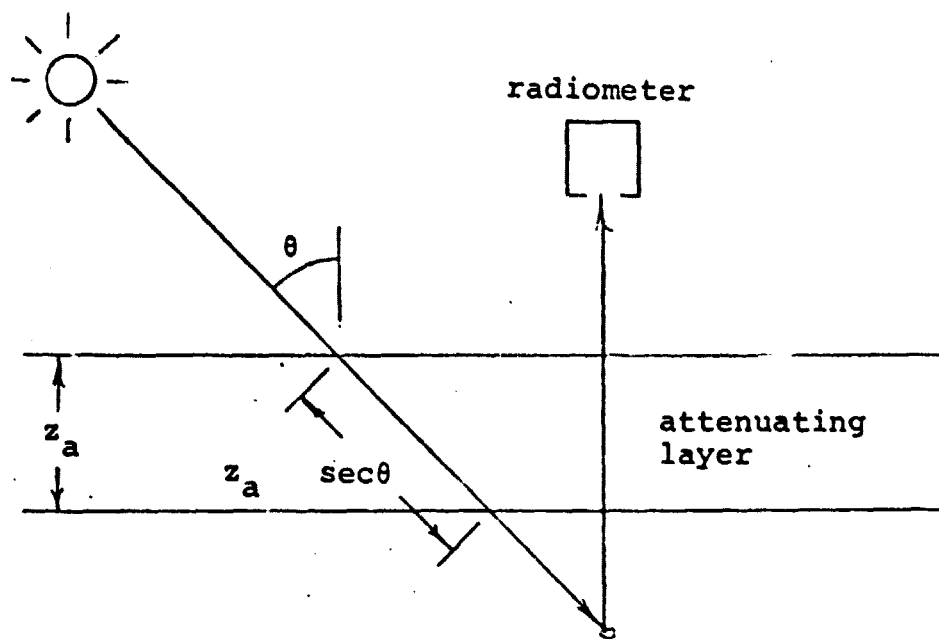


Fig. 20. Round-trip attenuation

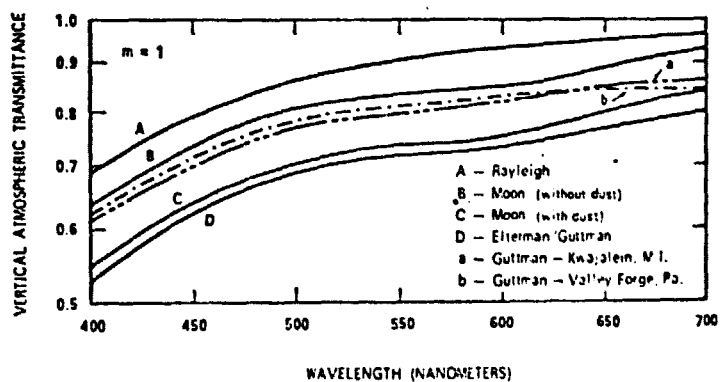


Fig. 21. Vertical beam transmittance of the atmospheric models (curves A, B, C, D) and as measured by Guttman (curves a and b). Applied Optics 7 (1968) p. 2377



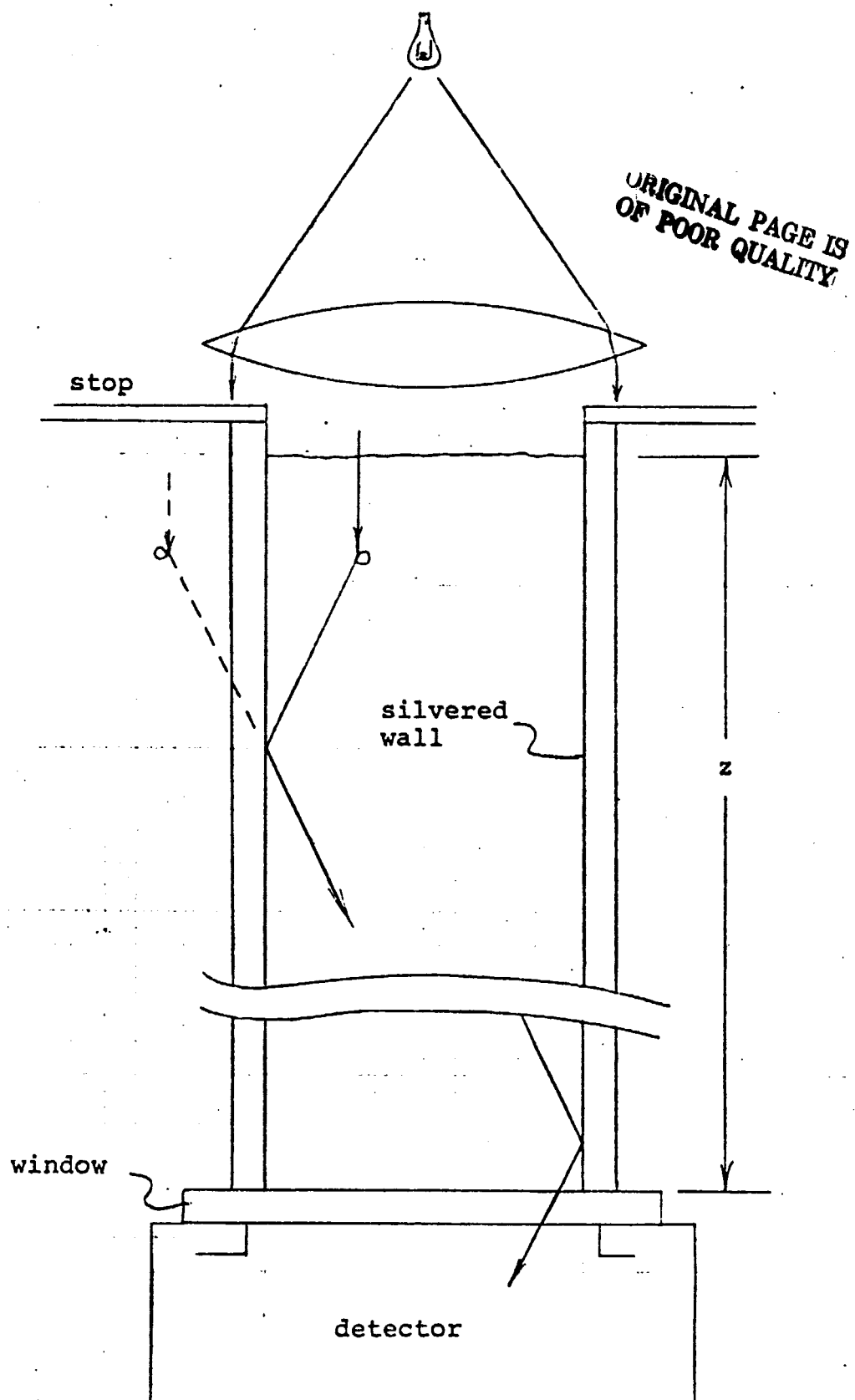


Fig. 22. Absorption cell for measuring pollutant transmittance  $\sqrt{T_p}$

Transmission varies approximately exponentially with distance  $z$ ,

$$\sqrt{T} = e^{-\alpha z}$$

but not exactly owing to multiple scattering in thick layers. The attenuation rate may be expressed

$$\alpha = \alpha_w + \alpha_o C$$

where  $\alpha_w$  is the attenuation in the water that dilutes the pollutant,  $\alpha_o$  is attenuation of undiluted pollutant, and  $C$  is its concentration. Combining these equations gives

$$T = e^{-\alpha_w z} e^{-\alpha_o (Cz)} \quad (14)$$

The factor  $Cz$  in parentheses is the area concentration of pollutant, so many grams per square meter, which says in effect that it makes no difference how the pollutant is distributed in depth. This is true so long as there is no chemical change that depends on concentration, as there is in the case of the DuPont acid dump. In the latter case,  $\alpha_o$  is a function of  $C$ . It is prudent not to assume that Eq. 14 holds over any wide range of  $C$  or  $z$  until verified in the laboratory. Over the intervals where it does hold, Eq. 14 provides an interpolation formula.

### 1.5.2 Surface Transmission

Near vertical transmission through the sea surface is given by

$$T_s = \left( \frac{4n_a n_w}{(n_a + n_w)^2} \right)^2 \left( \frac{n_a}{n_w} \right)^2 \quad (15)$$

The first factor is round-trip Fresnel reflection at the dielectric interface  $((1-r)^2$ , see Eq. 12). The second factor represents the

reduction of radiance rising out of the water due to angular spreading, Fig. 1. Using  $n_a = 1.0$ ,  $n_w = 1.34$  as before gives

$$T_s = (0.96) (0.56) = 53\% \quad (16)$$

The fact that the first factor has little effect implies that surface roughness is not a big factor in determining  $T_s$ , as shown in Fig. 18, except that patches of foam cause significant changes by scattering light upward and sideways.

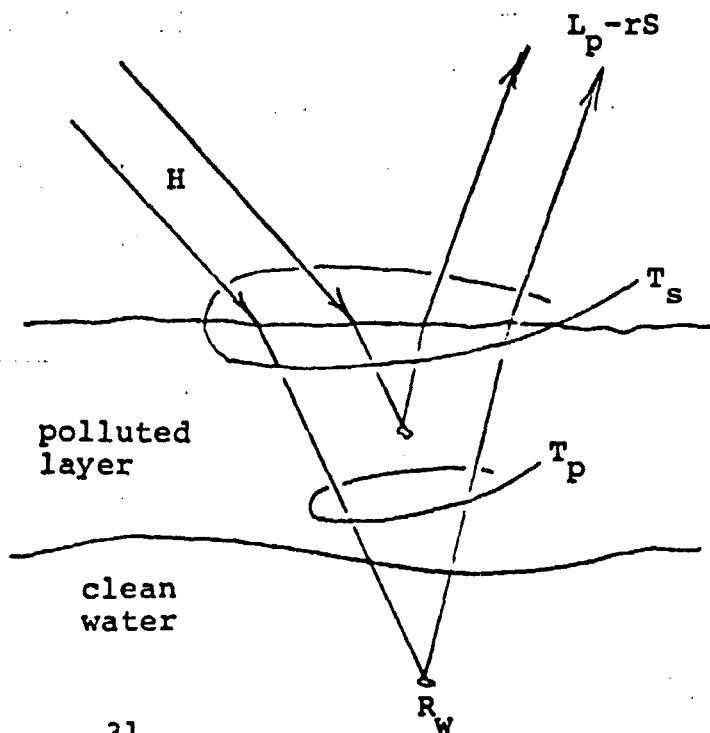
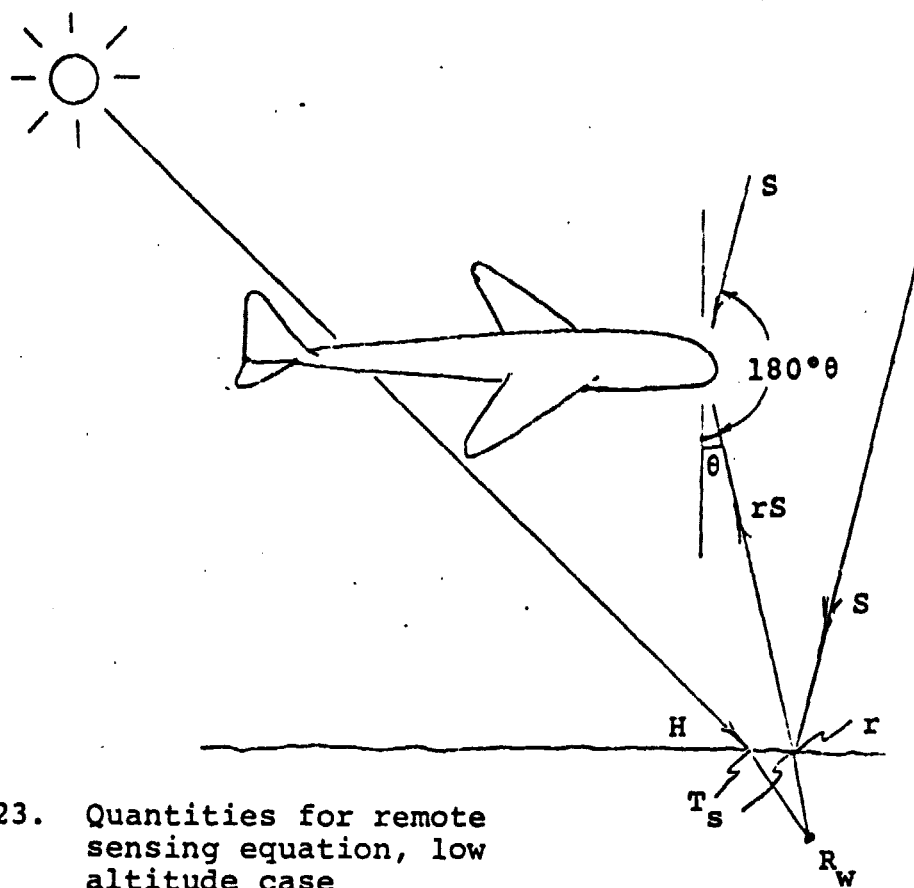
## 2.0 REMOTE SENSING EQUATIONS

This part of the report derives equations for determining pollutant concentration in two cases. The first is for a low altitude aircraft, and the second for high altitude, most likely a satellite.

### 2.1 Low Altitude

The significance of this case is that low altitude eliminates all atmosphere effects except reflected sky radiance, and we can deal with that by quite effective means. As discussed in Sec. 1.4, a good choice of aspect angle plus a polarization filter eliminates most of the interference from the sky when it is clear. At other times it is necessary to measure the spectral radiance of the sky directly with a sky radiometer so that the reflected radiance may be subtracted out of the sea data, Fig. 23. The best arrangement is to combine sea and sky radiometers into one instrument with the same detector and amplifier, so that any fluctuations in sensitivity affect both measurements equally. An optical switching or scanning arrangement causes the detector to look at the sky periodically between looks at the sea. (It need not look at the sky very often.) In any case, the pointing of the sky and sea radiometers must be at supplementary angles to the nadir as indicated by the reflection geometry in Fig. 23.

When the sea has normal roughness, the reflected image of the sky is blurred. This causes no problem when the sky is uniform, either clear or overcast. However, when the sky has broken clouds, the optics in the sky radiometer must blur the direct image in a manner that simulates the blurred reflected image that the sea radiometer sees. The proper amount of blur may be determined by measuring the angular diameters of the elliptical sun glint pattern.



The radiance seen over clean seawater is given by

$$L_c = HT_s R_w + rS \quad (17)$$

As Fig. 23 shows, the first term represents light that penetrates the water, and emerges, and the second term light that reflects from the surface. The latter is  $L_r$ , Eq. 11, either  $r_{||}S_{||}$  or  $r_{||}S_{||} + r_{\perp}S_{\perp}$  depending on whether a polarization filter is used. The first term in Eq. 17 is the larger by a factor of about three through most of the visible spectrum, but the two cross over near the red end, Figs. 8 through 10. Recall that every quantity in Eq. 17 is a spectrum. Their colors are as follows:

$$\left. \begin{array}{l} H \\ T_s \\ r \end{array} \right\} \text{white} \quad \begin{array}{l} R_w - \text{blue to green (water color)} \\ S - \begin{cases} \text{blue when clear} \\ \text{white when overcast} \end{cases} \end{array}$$

Also recall that Eq. 17 implies three spectral measurements of light intensity. The radiance of the sea and sky,  $L_c$  and  $S$  just discussed, and the irradiance  $H$ .

Now consider the changes that occur when the water is polluted. An oil slick changes  $r$  considerably, but this discussion is restricted to the case of soluble pollutants, which have negligible effect on  $r$  and merely change the color of the water. Fig. 24 shows the reflection and transmission factors that lead to the following equation:

$$L_p = HT_s (R_p + T_p R_w) + rS \quad (18)$$

The radiometer flying over a plume of pollution measures both  $L_c$  and  $L_p$  while also monitoring  $H$  and  $S$ . With these results,

Eqs. 17 and 18 are two equations to be solved for two unknowns. One unknown is the desired pollutant concentration implicit in its reflectance  $R_p$  and transmittance  $T_p$ . The other unknown can be one of the quantities  $R_w$  (water color),  $T_s$  (surface transmission), or  $rS$  (reflected sky), that is not easy to measure or estimate accurately. There are different cases in which any one of these may be poorly known. However, we postpone that discussion to complete the mathematics of the remote sensing equations.

When the color of the water  $R_w$  is unknown and eliminated from Eqs. 17 and 18, the result is Eq. 19 in the table on the following page. When surface transmission  $T_s$  is unknown, the result is Eq. 20. This equation has the added advantage that irradiance  $H$  is eliminated and therefore does not have to be measured. When reflected sky  $rS$  is unknown, the result is Eq. 21. In general one must solve the appropriate remote sensing equation 19, 20, or 21, by an iterative algorithm: assume a pollutant concentration, test the corresponding  $R_p(\lambda)$  and  $T_p(\lambda)$  in the equation, and evaluate the fit. Assume another concentration and evaluate, and so on to find a best fit.

A limiting case of interest occurs when the pollutant is a clear colored liquid, i.e.  $R_p = 0$ . In this case the remote sensing equations (19 - 21) become Eqs. 22 and 23 in the table.

Whenever  $L_p > L_c$ , this case cannot apply because the transmittance  $T_p$  has to be less than one. Eq. 22 is particularly nice because so many quantities drop out and therefore need not be measured.

Another limiting case is  $T_p = 1$ , i.e. the pollutant does not appreciably shade the water beneath it.\* This gives Eqs. 24 and 25.

---

\*Strictly speaking, if  $T_p = 1$ , then  $R_p = 0$ , but reflectances at sea are very small, so  $R_p$  can be .3% per steradian and  $T_p = 99.7\%$  is close enough to 1.

TABLE OF REMOTE SENSING EQUATIONS

Case	Quantities that drop out	Equation
General	$R_w$	$(L_p - rS) - (L_c - rS) T_p = HT_s R_p$ (19)
	$T_s, H$	$T_p + \frac{R_p}{R_w} = \frac{L_p - rS}{L_c - rS}$ (20)
	$r, S$	$T_p + \frac{R_p}{R_w} = 1 + \frac{L_p - L_c}{R_w HT_s}$ (21)
	$H, T_s, R_w$	$T_p = \frac{L_p - rS}{L_c - rS}$ (22)
Clear colored liquid $R_p = 0$	$r, S$	$T_p = 1 + \frac{L_p - L_c}{R_w HT_s}$ (23)
	$R_w, r, S$	$R_p = \frac{L_p - L_c}{HT_s}$ (24)
Thin milky liquid $T_p \approx 1$	$T_s, H$	$\frac{R_p}{R_w} = \frac{L_p - rS}{L_c - rS} - 1$ (25)



Equation 24 is a nice case because so few quantities are needed.

Let us return to the postponed question, which quantity should be treated as the second unknown? Much experimental work is needed to establish the circumstances reliably, but some general guidelines are as follows:

When the sea is fairly calm treat  $R_w$  (water color) as unknown and use Eq. 19. Sec. 1.3.2 discussed the fact that the color of seawater is not as obvious as it seems, and in fact measurements in situ are required to reliably determine  $R_w$ . Accordingly,  $R_w$  should be treated as the unknown whenever the sea is calm enough to be free of whitecaps so that  $T_s$  and  $r$  are fairly well known.

When the sea is choppy with foam and spray and the sky is uniform, assume  $T_s$  is unknown and use Eq. 20. One must work in a location where  $R_w$  has previously been established or else use only two colors, green and infrared, as discussed in Sec. 1.3.2. Foam and spray make it impossible to estimate either  $T_s$  or  $r$ . However,  $r$  may be measured indirectly leaving  $T_s$  as the unknown. For  $\lambda \geq 700$  nm,  $T_s$  is negligible, so Eq. 17 reduces to

$$L_c(\lambda > 700) = rS(\lambda > 700)$$

The sky radiometer measured  $S$  directly, and so  $r(\lambda > 700) = L_c/S$ . Moreover, the dependence of  $r$  on  $\lambda$  is very weak and known, so  $r$  is established throughout the spectrum leaving  $T_s$  as the unknown.

When the sky and sea are too complex to find a reasonable estimate of blurred reflected sky radiance, treat rS as the unknown and use Eq. 21. When both  $T_s$  and rS are indeterminate, rS should be treated as the unknown in the equations, because  $T_s$  is never too far from the factor  $(n_a/n_w)^2$  for the spread in solid angle. Other losses at the surface are not large (but not negligible either).

## 2.2 High-Altitude Sensor, Especially Satellite

Let  $L_c$  and  $L_p$  denote the spectral radiance (clean and polluted) measured by a sensor at high altitude. These quantities are related to the low-altitude measurements discussed in Sec. 2.1 as follows:

$$\left. \begin{aligned} L_c &= L_c \tau_a + L_a^* \\ L_p &= L_p \tau_a + L_a^* \end{aligned} \right\} \quad (26)$$

Here  $\tau_a$  is the one-way upward transparency of the air path and  $L^*$  the radiance (blue) of the air along the path. In other words, the luminance we wish to observe is attenuated by  $\tau_a$  and veiled by  $L^*$ . Unfortunately the path radiance  $L^*$  is about seven times larger than the terms with the desired information. This means that  $L^*$  must be subtracted off with considerable precision to avoid contaminating the ocean data with its errors.

Recall that  $L_c$  and  $L_p$  in these equations are given by Eqs. 17 and 18:

$$L_c = HT_s R_w + rS \quad (17)$$

$$L_p = HT_s (R_p + T_p R_w) + rS \quad (18)$$

In Sec. 2.1 we processed these two equations in three different ways appropriate to three different cases. However, in the high-altitude case, we always take the difference:

$$\Delta L = L_p - L_c = HT_s \tau_a (R_p + T_p R_w - R_w) \quad (27)$$

This not only eliminates the largest term  $L^*$  (and its uncertainty), but also  $rS$  in which neither  $r$  nor  $S$  is known very well from high altitude. (Sea state and low-lying hydrometeors may be in doubt.)

The factor  $H$  in Eq. 27 is irradiance at the sea surface, a quantity not normally available when the only measuring platform is at high altitude. Therefore, we replace it by the solar irradiance  $H_s$  measured at high altitude times some estimate  $\tau_a$  of downward atmospheric transmission:

$$H = H_s \tau_a$$

$$\Delta L = H_s (\tau_a \tau_a) T_s (R_p + T_p R_w - R_w)$$

It may seem that the product  $\tau_a \tau_a$  should be replaced by  $T_a$  to represent round-trip propagation as in Eq. 13 and other places. However, there is a subtle distinction between the two directions that needs to be emphasized. In the downward direction scattered light counts as long as it reaches the surface and thereby contributes to illumination. In the upward direction, this is not the case. As in Fig. 25, the polluted area is usually quite small compared with the altitude of the sensor. As a result the scattered light is diluted and completely lost in the scattered light from surrounding clean water. A distinction between polluted and clean areas is possible only in the unscattered light because the radiometer

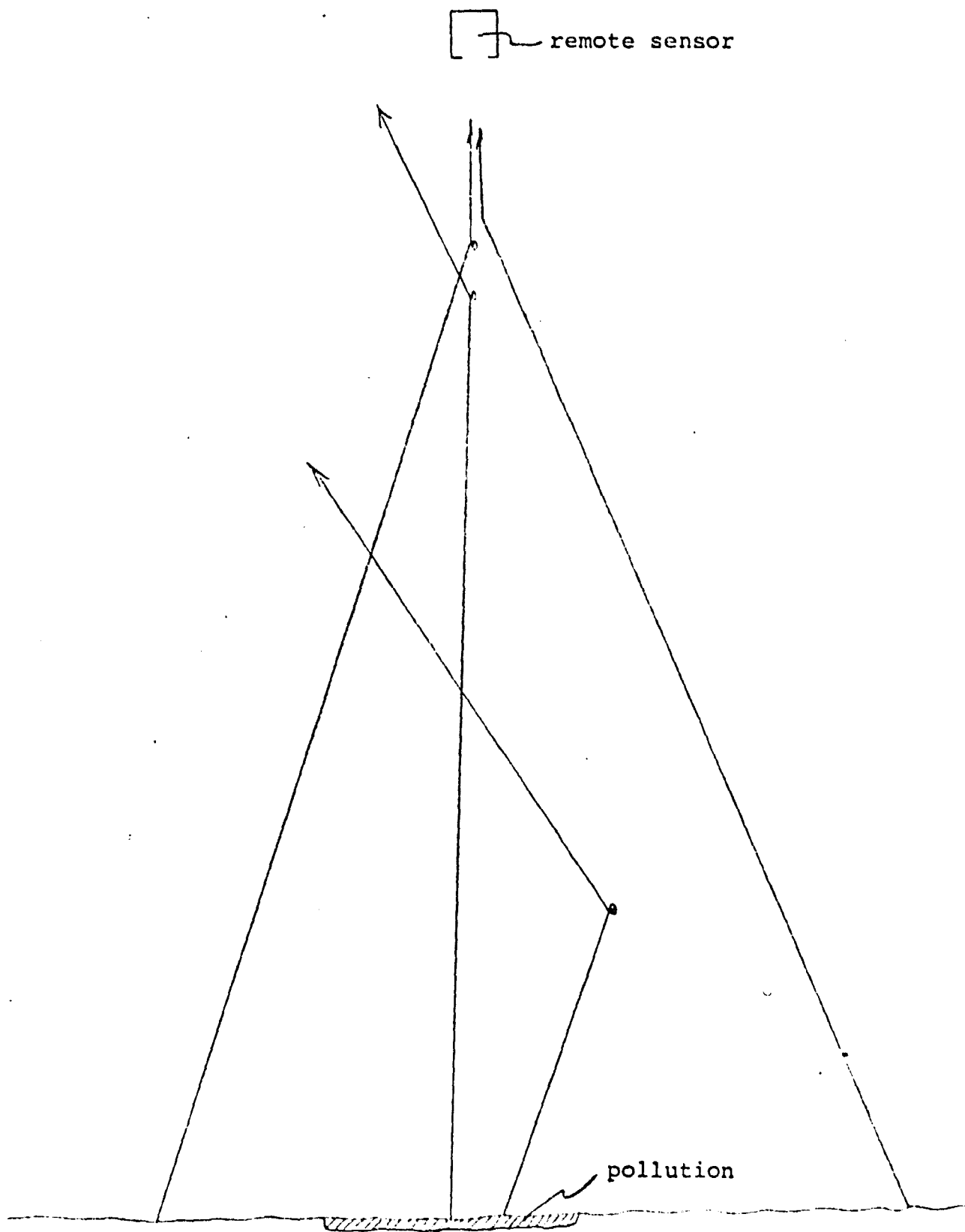


Fig. 25. Light from polluted area diluted by scattering

images them and compares radiance on each side of the image boundary. Thus light scattered in upward propagation drops out of the difference (Eq. 27) but unscattered light contributes, and we emphasize this with a change of notation:

$D_a - \tau_a$  including scattered light (D stands for down and diffuse)

$U_a - \tau_a$  excluding scattered light (U stands for up and unscattered)

Finally we have the remote sensing equation:

$$\Delta L = H_s D_a U_a T_s [R_p - (1 - T_p) R_w] \quad (28)$$

The evaluation of this expression is not nearly as satisfactory as the corresponding equation for low altitudes (choice of Eq. 19, 20, or 21). The direct measurements of H (at the surface) and S (sky) in the low altitude case have been replaced by quantities that involve indirect evidence and even conjecture. Clouds near the line of sight affect  $D_a$ . Foam, spray, and possibly other low-lying hydrometeors affect  $T_s$ . One can estimate a correction based on whiteness of the reflection from clear areas. However, it cannot be very accurate because one does not know how much of the whiteness to attribute to clouds (reduce  $D_a$ ), surface foam and spray (reduces  $T_s$ ), or to reflected sky (clouds), which has dropped out of Eq. 28.

## REFERENCES

- Ref. 1: N.G. Jerlov, Marine Optics, Elsevier Scientific Publishing, NY 1976
- Ref. 2: N.G. Jerlov and E.S. Nielsen, Optical Aspects of Oceanography, Academic Press, NY 1974
- Ref. 3: R.W. Austin, "The Remote Sensing of Spectral Radiance from Below the Ocean Surface," Chapter 14 in Ref. 2 (1974)
- Ref. 4: J.I. Gordon, SI069-20, University of California, San Diego (1969)